

Preparation and characterization of LaB₆ ultra fine powder by combustion synthesis

DOU Zhi-he, ZHANG Ting-an, ZHANG Zhi-qi, ZHANG Han-bo, HE Ji-cheng

Key Laboratory for Ecological Utilization of Multimetallic Mineral of Ministry of Education,
Northeastern University, Shenyang 110004, China

Received 25 November 2010; accepted 16 May 2011

Abstract: High-purity, homogeneous and ultra fine LaB₆ powders were prepared by combustion synthesis. The effects of reactant ratio and molding pressure on the phase and morphology of the combustion products were studied. The combustion products and leached products were analyzed by XRD, SEM and EDS. The results indicate that the combustion product consists of LaB₆, MgO and a little Mg₃B₂O₆. The combustion product becomes denser and harder when the molding pressure increases. The purity of LaB₆ is higher than 99.0%. The LaB₆ particle size is in range of 1.92–3.00 μm and the lattice constant of LaB₆ is $a=0.4148$ nm.

Key words: combustion synthesis; lanthanum hexaboride; Mg₃B₂O₆

1 Introduction

Lanthanum hexaboride (LaB₆) with divalent rare-earth cubic hexaborides [1] has high melting point (2715 °C), high hardness, high chemical stability [2] and the other special peculiarities [3] such as high and constant electrical conductivity, low electronic work function, low expansion coefficient and high neutron absorbability [4]. At the same time, LaB₆ has lower evaporation rate and more carbon fouling resistance than LaB₆ as the cathode emission material. Now LaB₆ has been widely used in metallurgy [5–6], wave-absorbing materials, cathode emission materials [7–8], nuclear industry and so on [9]. LaB₆ is also a promising refractory ceramic [10–12]. The major methods of preparing LaB₆ powders include direct combination method of B and La, carbothermal reduction method and boron carbide synthesis method [13]. The direct elements combination method of preparing LaB₆ powders cannot be used for industrial production because of the high cost. At present, the carbothermal reduction method and the boron carbide method are widely used in industry. However, the powders prepared by these methods have a larger particle size, a lower purity (because of higher

content of free carbon in LaB₆ products) and a poorer sintering property. Although the nano-sized powders of LaB₆ could be prepared by chemical vapor deposition (CVD) [9], the yield was lower for a longer production process. Therefore, it is important to develop an efficient method to prepare LaB₆ powders with high purity and small particle size. Combustion synthesis has attracted much attention to the synthesis of novel materials because of high reaction speed, high temperature, high cooling speed, simple equipment involved and low energy consumption [14]. The object of this work is to prepare LaB₆ ultra powders with high purity and small particle size from Mg-B₂O₃-La₂O₃ system by combustion synthesis method [15].

2 Experimental

2.1 Preparation

The materials included magnesium powder with 99% purity and particle size from 74 to 149 μm, B₂O₃ powder with 98% purity and particle size smaller than 149 μm and La₂O₃ powder with 99.5% purity and particle size smaller than 149 μm. The materials were weighed stoichiometrically according to the following equation:



Detailed reactant ratio is listed in Table 1.

Table 1 Combustion synthesis reaction condition

Sample No.	Pressure/MPa	Reactant ratio of Mg
1	5	5% more than stoichiometry
2	10	10% more than stoichiometry
3	20	15% more than stoichiometry

The powders were mixed by milling for 24 h. Subsequently, the mixed powders were pressed into cylinders under pressure of 5–20 MPa. The cylindrical bulks were then placed in the open equipment to perform the combustion synthesis. The ignitor of magnesium powders was placed on the surface of the bulk sample. The combustion products were acid-leached and LaB_6 powders were obtained after filtration and drying.

2.2 Analytical methods

The phase compositions of the combustion product and the acid-leached product were analyzed by X-ray diffractometry (Model D8 Bruke German; working conditions: Cu $K_{\alpha 1}$, 40 kV, 40 mA). The powder morphology was observed using scanning electron microscopy (SEM, Model Hitachi S-4700, Japan). The powder element composition was analyzed by energy dispersive spectrometry (EDS, Model AMETEKEDAX GENESIS, USA). The molar ratio of B to La was determined by inductively coupled plasma atomic emission spectrometry (Model ICP-Prodigy, Optima 4300 DV, Lehman USA).

3 Results and discussion

3.1 XRD analysis of combustion product

Because Mg volatilizes during the combustion reaction process with reaction temperature rising rapidly, there are some brown MgO particles (determined by the XRD) formed attached to the inner wall of the reaction chamber. Figure 1 shows the XRD pattern of the combustion product. It is seen that the combustion product includes $\text{Mg}_3\text{B}_2\text{O}_6$ besides MgO and LaB_6 . The reaction mechanism can be expressed as



The by-product $\text{Mg}_3\text{B}_2\text{O}_6$ appears because of reaction (2). The reasons can be explained as [14–15]: 1) Mg partly volatilizes to form MgO in oxidation due to the high reaction temperature during the self propagating high temperature synthesis (SHS) process, MgO reacts with the local surplus B_2O_3 to form

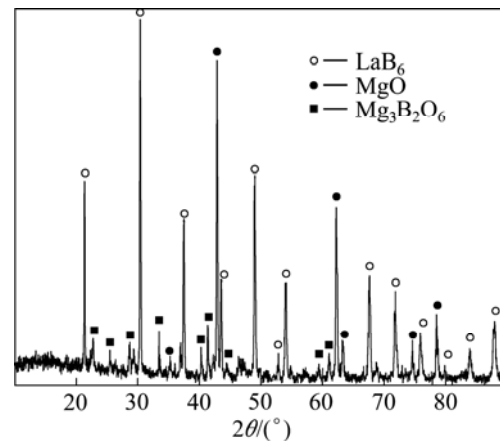


Fig. 1 XRD pattern of combustion product

$\text{Mg}_3\text{B}_2\text{O}_6$; and 2) there is a long heating process at the beginning of SHS reaction, promoting the formation of $\text{Mg}_3\text{B}_2\text{O}_6$.

Based on the quantitative analysis of XRD results, it can be concluded that the content of by-product $\text{Mg}_3\text{B}_2\text{O}_6$ decreases with increasing Mg reactant ratio. The excessive Mg could make up for the Mg volatilization loss, and the reduction degree of B_2O_3 and La_2O_3 seen from Eq. (1) is enhanced. Therefore, the yield of LaB_6 increases, indicating that the optimum Mg ratio should be 10% more than stoichiometry.

3.2 Microstructure of combustion products

The SEM images of the combustion products are shown in Fig. 2. It can be seen in Fig. 2 that the combustion products present black-brown, obviously layered and full of cavities, and the volume expands. Figure 2 shows that there are soft aggregates in sample 1 which could be ground easily. But sample 3 synthesized under molding pressure of 20 MPa is denser/harder and has no voids and layer structure. This can be expressed as [15]: 1) the combustion of Mg- B_2O_3 - La_2O_3 system is a periodic oscillation process which promotes the formation of layer structure; 2) the volatilization of Mg and the discharge of gas result in some cavities and volume expansions in the combustion products. The combustion products become denser and less layered when the reactant ratio of Mg and the molding pressure increase.

The EDS analyses of the combustion product are shown in Fig. 3. The spherical particles are MgO (see Fig. 3(a)). The aggregates distributing around MgO are mainly $\text{Mg}_3\text{B}_2\text{O}_6$ and LaB_6 (see Fig. 3(b)).

3.3 XRD analysis of acid-leached products

It can be seen that the combustion product consists of LaB_6 , MgO and $\text{Mg}_3\text{B}_2\text{O}_6$. $\text{Mg}_3\text{B}_2\text{O}_6$ and MgO are solvable in hydrochloric acid, while LaB_6 is unsolvable,

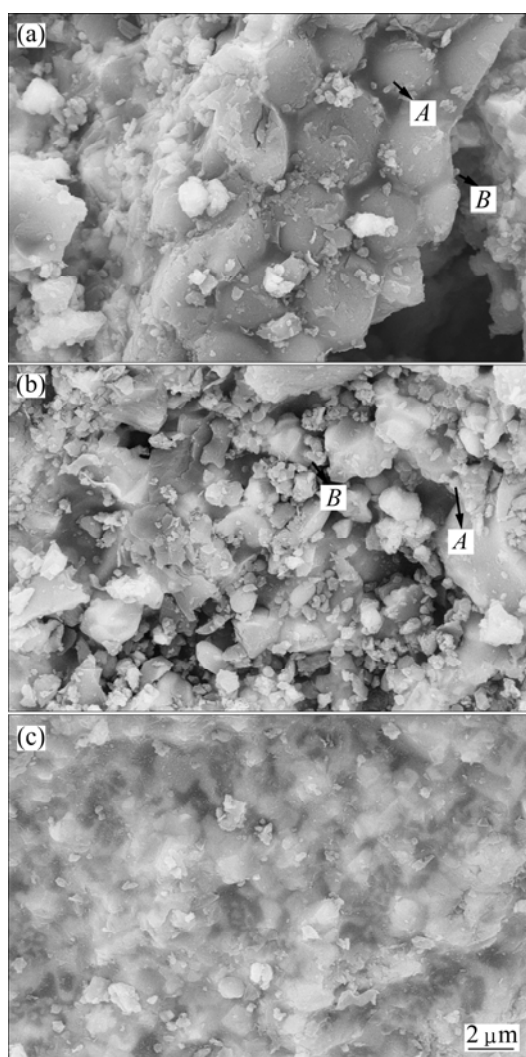


Fig. 2 SEM photographs of combustion product samples: (a) Sample 1; (b) Sample 2; (c) Sample 3

so the combustion product could be acid-leached with HCl acid of 4 mol/L in a water bath at 60–80 °C for more than 4 h with mechanical agitation of 300 r/min.

The XRD pattern of leached product sample 3 is shown in Fig. 4. It indicates that high HCl concentration, water bath temperature and high agitation speed could favor the removal of the impurity. Pure powders of LaB_6 are obtained after leaching, the purity of which is higher than 99.0%. Table 2 shows the chemical analysis results of impurities determined by inductively coupled plasma atomic emission spectrometry (ICP–prodigy). The mole ratio of B to La is 6, which is also determined by ICP.

Table 2 Impurity in LaB_6 powders (mass fraction, %)

Mg	Cr	Al	Ti
0.3	0.02	0.03	0.03
Ni	Fe	Mn	Si
0.01	0.1	0.1	0.03

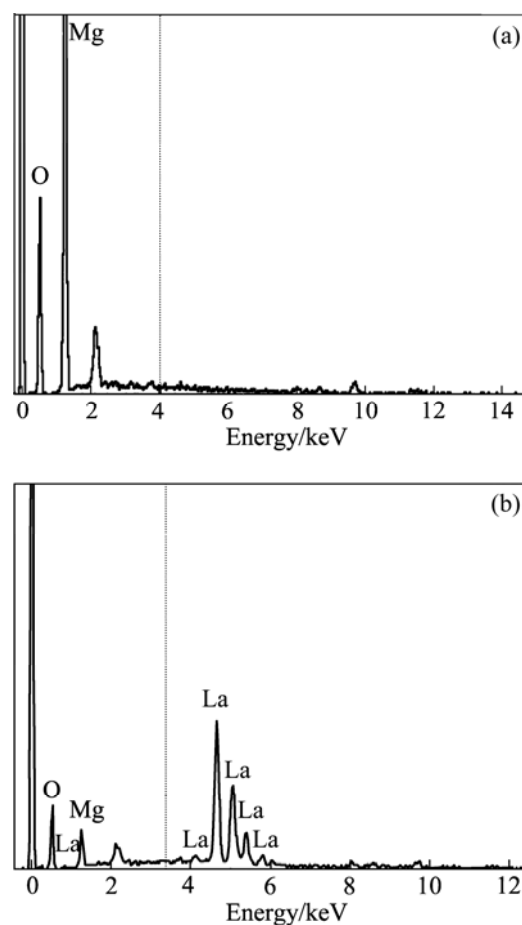


Fig. 3 EDS analyses of combustion products: (a) Point A in sample 1; (b) Point B in sample 1

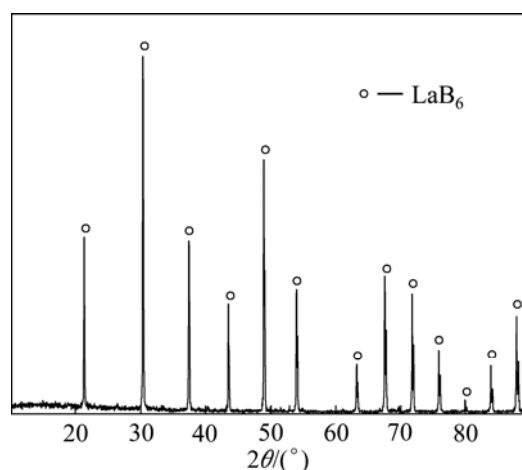


Fig. 4 XRD pattern of leached product sample 3

3.4 SEM analysis of acid-leached products

The SEM images of leached products are shown in Fig. 5. It can be seen from Fig. 5 that the size of LaB_6 particle ranges from 1.92 to 3.00 μm and distributes evenly. The single particle is cubic, anastomosed to the cubic crystal type of LaB_6 . In Figs. 5(a)–(c), LaB_6

particles become finer with increasing molding pressure, respectively. There are some particles aggregate (see Fig. 5(a)), but the soft particle aggregations do not exist in samples 1 and 3 under higher molding pressures of 10 and 20 MPa. The growth of LaB_6 grain is prevented at higher pressure. The average grain size is about $3\ \mu\text{m}$ at the pressure of $5\ \text{MPa}$, and then the average grain size is smaller than $2.0\ \mu\text{m}$ when the molding pressures are 10 and 20 MPa. Reaction temperature increases with increasing pressure. The high reaction temperature could favor the synthesis of LaB_6 .

The TEM image and diffraction design of LaB_6 are shown in Fig. 6. It indicates that the LaB_6 particles are polycrystalline, the lattice constant is $a=0.415\ 0\ \text{nm}$, which anastomoses to $a=0.415\ 2\ \text{nm}$.

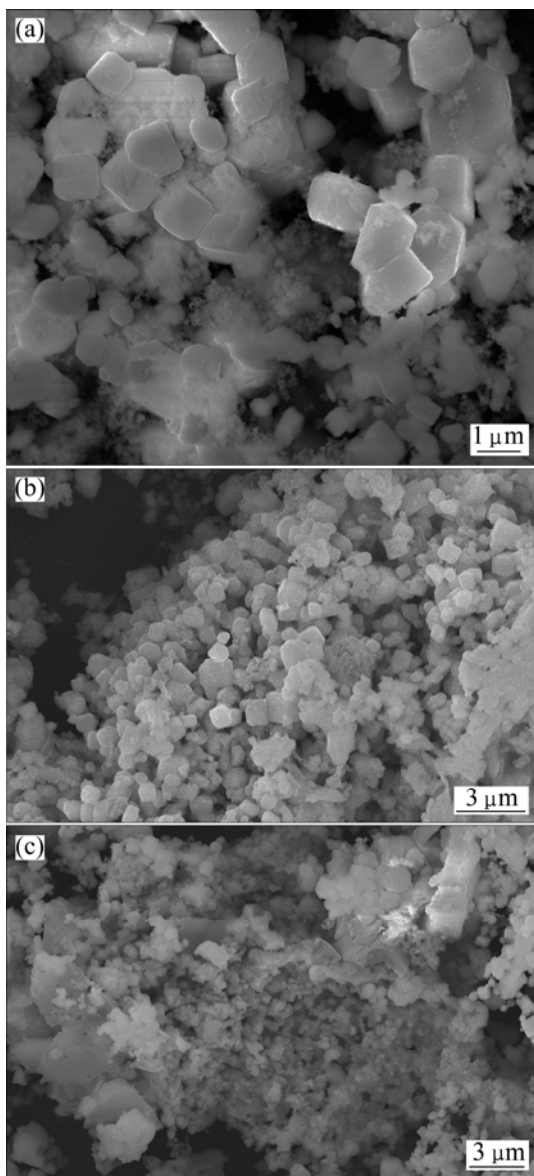


Fig. 5 SEM images of different LaB_6 powders: (a) Sample 1; (b) Sample 2; (c) Sample 3

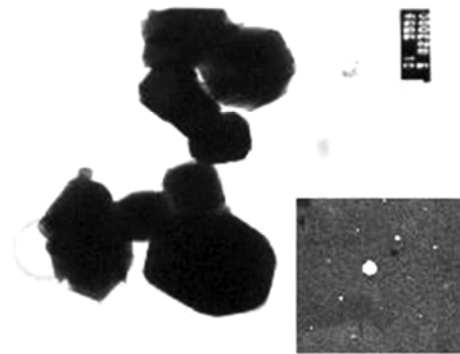


Fig. 6 TEM image and diffraction design of LaB_6

4 Conclusions

1) The combustion product consists of LaB_6 , MgO and $\text{Mg}_3\text{B}_2\text{O}_6$. The combustion products are unconsolidated and layered. The combustion product becomes denser and harder when the molding pressure increases.

2) The leached product is cubic, anastomosed to the cubic crystal type of LaB_6 . The purity of LaB_6 is higher than 99.0%. The size of LaB_6 particle is $1.92\text{--}3.00\ \mu\text{m}$ and the lattice constant of LaB_6 is $a=0.414\ 8\ \text{nm}$.

References

- [1] ZHANG Mao-feng, YUAN Liang, WANG Xiao-qing, WANG Xu-yang, WU Xue-ying, WANG Hai-zhen, QIAN Yi-tai. A low-temperature route for the synthesis of nanocrystalline LaB_6 [J]. *Journal of Solid State Chemistry*, 2008, 181(2): 294–297. (in Chinese)
- [2] ZHANG Ting-an, DOU Zhi-he. Preparation of LaB_6 micropowder by high-temperature self-propagating synthesis and characterization[J]. *Journal of Northeastern University (Natural Science)*, 2004, 25(1): 271–273. (in Chinese)
- [3] PADERNO V, PADERNO Y, BRITUN V. Features of the real structure of lanthanum hexaboride single crystals [J]. *Journal of Alloys and Compounds*, 1995, 219(94): 228–231.
- [4] ZHANG Ting-an, HE Ji-cheng. Ceramic micro-powders of TiB_2 and LaB_6 by SHS metallurgy [M]. Shenyang: Northeastern University Press, 1999: 69–147. (in Chinese)
- [5] TAKAHO T, EISUKE B, SHICHO K. Preparation of EuB_6 single crystal [J]. *Cryst Growth*, 1977, 40(2): 125–128.
- [6] TAKAHASHI T, KUNII S. Single crystal growth and properties of incongruently melting ThB_6 , DyB_6 , HaB_6 , YB_6 [J]. *Solid State Chem*, 1977, 133(1): 198–200.
- [7] BAT'KO, BAT'KOVA M, FLACHBART K, FILIPPOV V B, PADERNO Y B, SHICEVALOVA N Y, WAGNER T. Electrical resistivity and superconductivity of LaB_6 and LuB_{12} [J]. *J Alloys Compd*, 1995, 217(2): L1–L3.
- [8] ZHENG Shu-qi, MIN Gunang-hui, ZOU Zeng-da, YU Hua-shun, ZHANG Chuan-jiang. Fabrication process of LaB_6 powder by borothermic reduction method[J]. *Journal of the Chinese Ceramic Society*, 2001, 29(2): 129–131. (in Chinese)
- [9] SHI Qing-xuan, LIN Zu-lun, LI Jian-jun, CHEN Ze-xiang. LaB_6 thin films prepared by electron beam evaporation and its property[J].

- Chinese Journal of Electron Devices, 2007, 30(3): 745–747. (in Chinese)
- [10] MATSUSSHITA J, MORI K, NISHI Y, SAWADA Y. Oxidation of calcium boride at high temperature[J]. Mater Syn Pro, 1986(6): 407–410.
- [11] PADERNO V B, PADERNO Y B, MARTYNYENKO A N, VOLKOGON V M. Effect of production procedure on structure formation and fracture of $\text{CaB}_6\text{-TiB}_2$ [J]. Pseude alloy Poroshk Metal, 1992, 10(1): 52–55. (in Russian)
- [12] SHIGEKI O. Preparation of CaB_6 crystal by the floating zone method[J]. Journal of Crystal Growth, 1998, 192(1–2): 346–349.
- [13] ZHANG Ting-an, DOU Zhi-he, YANG Huan, DING Qian-li. Preparation of boron carbide by magnesium reducing-SHS[J]. Journal of Northeastern University (Natural Science), 2003, 24(10): 936–939. (in Chinese)
- [14] DOU Zhi-he, ZHANG Ting-an, HOU Chuang, XU Shu-xiang, YANG Huan, LI Huang. Elementary research on CaB_6 prepared by SHS[J]. The Chinese journal of Nonferrous Metals, 2004, 14(2): 322–326. (in Chinese)
- [15] WANG Y L, ZHANG T A, YANG H, WEI S C. Preparation of tungsten powder by SHS with a reduction process[J]. Journal of Advanced Materials, 2004, 36(2): 44–48.

燃烧合成法制备 LaB_6 超细粉末及表征

豆志河, 张延安, 张志琦, 张含博, 赫冀成

东北大学 多金属共生矿生态化利用教育部重点实验室, 沈阳 110004

摘要: 采用燃烧合成法制备高纯超细 LaB_6 粉末。考察反应物配比和制样压力等条件对燃烧产物相组成和微观结构的影响, 利用 XRD、SEM 和 EDS 等技术对燃烧产物和浸出产物进行表征。结果表明, 燃烧产物由 LaB_6 、 MgO 和少量 $\text{Mg}_3\text{B}_2\text{O}_6$ 组成。随着制样压力的增加, 燃烧产物变得致密坚硬。 LaB_6 的纯度高于 99.0%, 其粒度为 1.92–3.0 μm , 晶格常数 $a=0.4148\text{ nm}$ 。

关键词: 燃烧合成; LaB_6 ; $\text{Mg}_3\text{B}_2\text{O}_6$

(Edited by FANG Jing-hua)